Catalysis Letters 51 (1998) 139–147

Density functional theory (DFT) and microcalorimetric investigations of CO adsorption on Pt clusters

R.M. Watwe, B.E. Spiewak [*], R.D. Cortright and J.A. Dumesic [**]

Department of Chemical Engineering, University of Wisconsin, Madison, WI 53706, USA

Received 15 December 1997; accepted 25 February 1998

Microcalorimetric measurements were conducted at 573 K of CO adsorption on Pt clusters supported in L-zeolite. The measured heat of CO adsorption is 175 kJ/mol, and the heat decreases to 90 kJ/mol near saturation coverage. Quantum chemical calculations were performed using density functional theory to study the interaction of CO with 10-atom Pt clusters. The heat of CO adsorption on atop-sites is calculated to be 209 kJ/mol, while a lower heat of 142 kJ/mol is calculated for CO on bridge-sites. These values decrease to 197 and 102 kJ/mol for population of two atop-sites and two bridge-sites, respectively, on the same Pt_{10} cluster. The heat of adsorption decreases to 157 kJ/mol when six CO molecules adsorb on six atop-sites of the cluster. The calculated initial heat of CO adsorption on Pt_{10} clusters is in agreement with experimental and theoretical values reported for CO adsorption on Pt single-crystal surfaces. The higher heat of CO adsorption at atop-sites may be caused by more σ-donation from CO to sp orbitals of Pt for atop-sites. The heat of CO adsorption on bridge-sites becomes higher on negatively charged platinum clusters. The calculated C–O stretching frequencies for charged and neutral platinum clusters agree with experimental data.

Keywords: microcalorimetry, carbon monoxide, adsorption, platinum, DFT

1. Introduction

Quantum chemical calculations are increasingly being applied to predict the interactions of adsorbates with catalytic sites [1]. Application of these theoretical approaches requires careful comparison of the predictions with experimental data, to determine which level of theory is sufficient to describe the active sites at an acceptable computational time (e.g., the functionals used to describe electron exchange and correlation, the basis sets used, the number of atoms in the cluster, the symmetry constraints imposed on the cluster). In the present investigation, the interaction of carbon monoxide with a platinum cluster containing ten atoms was studied using both theoretical and experimental techniques. Density functional theory (DFT) methods were used to predict the interactions of CO with these Pt_{10} clusters. Such DFT methods have proven to be useful to predict accurate geometries and reasonable energetics for molecules containing transition metals [1–5]. The currently available DFT methods use few semiempirical parameters in conjunction with more advanced functionals to give an adequate description of nonlocal effects in electron exchange and correlation interactions.

In addition to being computationally tractable, the Pt_{10} clusters are also of interest as models of highly dispersed platinum catalysts. For example, small platinum clusters supported in neutralized L-zeolite have been shown to have novel catalytic properties for various hydrocarbon reactions, such as the aromatization of hexane to benzene [6–9]. Platinum clusters supported in L-zeolite have also been suggested to possess chemisorption properties that are different compared to larger platinum particles on other supports [10]. These platinum clusters in L-zeolite contain a limited number of platinum atoms (e.g., 5–10 atoms) [11,12], and the unique catalytic and chemisorptive properties of these clusters have been attributed to the small cluster size, as well as to possible interactions of these clusters with the zeolite support [8].

We will show in the present paper that the experimentally measured initial heat of CO adsorption on Pt/L-zeolite (∼175 kJ/mol) is in general agreement with the predictions of DFT calculations for the adsorption of CO on atop-sites of 10-atom platinum clusters. Furthermore, adsorption of CO on atop-sites is more stable than adsorption on bridge-sites by 65 kJ/mol. We also report how the adsorption energy, the geometrical parameters, and C–O stretching frequency of chemisorbed CO may depend on the charge of the platinum cluster.

2. Methods

2.1. Density functional theory calculations

The density functional theory calculations were carried out using DEC workstations, with PS-GVB software (Schrodinger, Inc.) [13]. This software uses a pseudospectral method to evaluate the various integrals. It combines both a basis set and a physical space grid, thus retaining the speed of discrete methods and the smoothing properties of continuous functions. The chosen DFT

---

[*] Present address: 3M Corporation, St. Paul, MN 55144, USA.

[**] To whom correspondence should be addressed.

method uses a hybrid method employing Becke's three-parameter approach, B3LYP [14]. This functional combines the exact HF exchange, Slater's local exchange functional, Becke's 1988 nonlocal gradient correction to the exchange functional, with the correlation functionals of Vosko–Wilk–Nusair (VWN) and Lee–Yang–Parr (LYP).

The basis set employed in all calculations (LACVP**) uses an effective core potential on all Pt atoms, developed at Los Alamos National Laboratory by Hay and Wadt [15]. The electrons treated explicitly on Pt are the outermost core and valence electrons ($5s^25p^65d^96s^1$), with the remaining core electrons treated with effective core potentials which account for the mass–velocity and relativistic effects. The inclusion of outermost core electrons with the valence electrons is necessary because these core orbitals have similar sizes as the valence orbitals. The C and O have been treated with the 6-31G** basis set [16], with all electrons being treated explicitly.

The heat of adsorption ($-\Delta H_{\text{ads}}$) is defined as

$$-\Delta H_{\text{ads}} = (E_{\text{cluster}} + H_{\text{adsorbate}}) - E_{\text{cluster/adsorbate}},$$

where $E_{\text{cluster/adsorbate}}$ is the total energy of the adsorbate on the cluster, E_{cluster} is the total energy of the bare cluster (Pt_{10}), and $H_{\text{adsorbate}}$ is the enthalpy of the adsorbate (CO). It is convenient to define the heat of adsorption as $-\Delta H_{\text{ads}}$, and a positive heat of adsorption indicates a favorable process.

Total energies were calculated for CO, Pt_{10} and CO–Pt_{10} by conducting full geometry optimizations. The Pt–Pt bond distances in these geometry optimizations were not constrained, since relaxation and adsorption-induced reconstruction effects are common for small particles [17–19]. For completeness, however, we also studied CO adsorption on a Pt_{10} cluster for which the Pt–Pt bonds were fixed at the bulk distance 2.77 Å, and the heat of adsorption obtained was larger by ~20–25 kJ/mol than the result obtained without constraints.

The total energies calculated after geometry optimizations were corrected for basis set superposition error (BSSE) using Boys–Bernardi counterpoise calculations for all adsorbate/cluster models [20]. This correction is ~10–12 kJ/mol per bond between the adsorbate and the cluster.

Stretching frequencies of the C–O bond were calculated for various clusters. The calculated value of C–O stretch for molecular CO was 2213 cm^{-1}. This frequency was scaled by 0.968 to match the experimental gas-phase value for CO which is 2143 cm^{-1} [21]. The frequency for chemisorbed CO was also scaled by the same factor from the calculated value for all clusters.

2.2. Microcalorimetry

Microcalorimetric measurements were performed at 573 K using a high-temperature heat-flux microcalorimeter [22]. The microcalorimeter was connected to a gas handling system and a volumetric system (dynamic vacuum of 10^{-7} Torr) employing Baratron capacitance manometers for precision pressure measurement ($\pm 0.5 \times 10^{-4}$ Torr). The maximum apparent leak-rate of the volumetric system (including the microcalorimetric cells) was ca. 10^{-6} Torr/min in a system volume of approximately 70 cm^3 (i.e., 10^{-6} μmol/min).

The microcalorimetric procedures used in this study have been described in detail elsewhere [22–24]. Briefly, each sample was treated *ex situ* in ultra-pure flowing gases, and then sealed in a Pyrex capsule. The Pyrex capsule formed in this manner was then broken in a special set of microcalorimetric cells [24], after the sample had attained thermal equilibrium with the microcalorimeter. In this manner, it was possible to expose the clean sample to CO without excessive surface contamination that can accumulate during the long times (ca. 5–10 h) required for thermal equilibration of sample in the microcalorimeter. After the capsule had been broken, microcalorimetric data were collected by sequentially introducing small doses (1–10 μmol quantities) of adsorbate onto the platinum sample (0.25–1.0 g) until it became saturated. The resulting heat response for each dose was recorded as a function of time and integrated to determine the energy released (mJ). The amount of gas adsorbed (μmol) was determined volumetrically from the dose and equilibrium pressures, and the system volumes and temperatures. The differential heat of adsorption was then calculated as a function of the amount adsorbed.

Sample treatments for the microcalorimetric experiments were performed in a Pyrex treatment cell equipped with a Pyrex NMR tube for sealing the samples [24]. Ultrahigh purity hydrogen (99.999%, Liquid Carbonic), used for sample treatments, was purified by diffusion through a palladium alloy thimble. Ultrahigh purity helium (99.999%, Liquid Carbonic), also used for sample treatments, was purified by passage over heated (473 K) copper turnings and activated molecular sieves (13X) cooled to 77 K. These gases were further purified by passage through a bed of reduced Oxy-Trap (Alltech Association, Inc.) and a bed of reduced iron catalyst to remove oxygenates. Carbon monoxide was purified by passage over heated (473 K) quartz wool to decompose metal carbonyls and activated molecular sieves (13X) maintained at room temperature.

The neutralized Pt/L-zeolite sample used in this study is the 1 wt% Pt/BaK-L zeolite sample studied by Sharma et al. [25]. This sample was prepared by incipient wetness impregnation of $Pt(NH_3)_4(NO_3)_2$ on a neutralized L-zeolite support (6.9 wt% Ba, 9.7 wt% K, Si/Al ~ 3.5, Linde Corp.), as described elsewhere [25]. The impregnated catalyst was dried at 393 K and calcined at 523 K. Prior to microcalorimetric studies, the sample was heated slowly (0.8 K/min) in flowing hydrogen to 673 K, reduced for 3 h at this temperature, and subsequently purged with flowing helium for 2 h at this temperature to remove adsorbed hydrogen. The reduced sample was then isolated in 350 Torr of helium at room temperature, and sealed in the Pyrex NMR tube (1.5 cm o.d. × 4 cm long) attached to the side of the treatment cell.

3. Results and discussion

3.1. Microcalorimetry

Microcalorimetric results for carbon monoxide adsorption on 1 wt% Pt/BaK-L zeolite at 573 K are shown in figure 1. Also shown, for comparison, are microcalorimetric data obtained by Sharma et al. for CO adsorption at 403 K on the same sample [25]. At 573 K, the initial heat of CO adsorption is ca. 175 kJ/mol. The differential heat decreases with increasing CO coverage until a saturation coverage of ca. 30 μmol/g is reached. In contrast, an initial heat of ca. 130 kJ/mol is measured for CO adsorption at 403 K on the same sample. The differential heat decreases gradually with increasing coverage for the first 18 μmol/g of CO uptake. At higher coverages, the differential heat decreases more rapidly until the surface becomes saturated at a final CO coverage of ca. 23 μmol/g. These results suggest that CO does not equilibrate with the sample at the lower adsorption temperature (i.e., 403 K). In fact, the rate constant for CO desorption at 403 K is expected to be very low ($\sim 10^{-10}$ s^{-1}) for a desorption energy of 175 kJ/mol, using a standard preexponential factor of 10^{13} s^{-1}. The low heats of adsorption (100–130 kJ/mol) measured at 403 K for this sample thus represent average adsorption heats, caused by chromatographic adsorption of CO in the catalyst bed. It is possible that complete equilibration of CO with Pt does not take place even at 573 K (desorption rate constant of 10^{-3} s^{-1}), and therefore we conclude that the initial heat of CO adsorption on Pt clusters in L-zeolite is higher than 175 kJ/mol.

The aforementioned value of the initial heat of CO adsorption on Pt/L-zeolite is near the range of values reported for CO adsorption on various single-crystal platinum surfaces. The initial heats of CO adsorption on Pt(110) and the hexagonal and (1×1) phases of Pt(100) have been measured to be 183, 180 and 225 kJ/mol, respectively [26,27]. The initial heat of CO adsorption on Pt(111) was reported to be 180 kJ/mol [28].

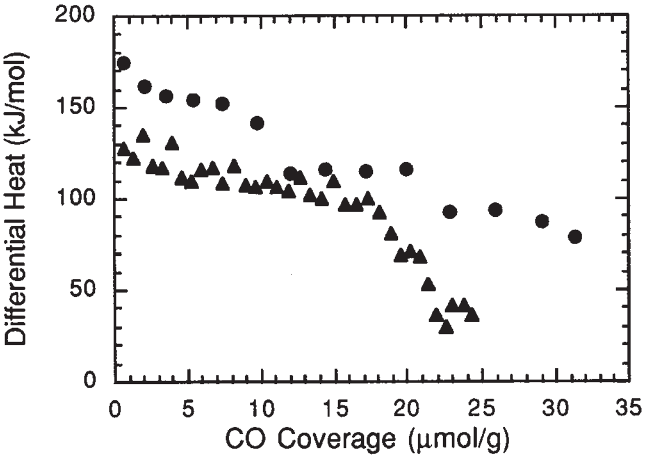

Figure 1. Microcalorimetric results for CO adsorption on 1% Pt/BaK-L zeolite at 403 K (▲) and 573 K (●).

Mojet and Koningsberger have reported CO-induced disruption of small Pt particles in K-LTL zeolite at high CO pressures (375 Torr) [12]. An earlier study has shown that neutral Pt carbonyl species may be formed from Pt particles upon CO adsorption at high CO pressures, whereas IR data of CO adsorbed on Pt/K-L zeolite at low pressures (0.76 Torr) did not show evidence for the disruption of Pt particles [29]. These observations agree with IR data of CO adsorption on the Pt/K(Ba)-L zeolite used in this study [30], i.e., Pt carbonyl species are not formed upon exposure of the Pt particles to CO at low pressures. Since the microcalorimetric measurements of the present study have been performed at low CO pressures (lower than ∼4 Torr), we attribute the measured energy change to the heat of CO adsorption, without disruption of Pt particles to form Pt carbonyl species.

3.2. Density functional theory calculations: Pt_{10}

The Pt_{10} cluster used in this study has ten atoms arranged into three layers resembling (111) planes, as shown in figure 2. This cluster has three-fold, two-fold and atop-adsorption sites. The Pt–Pt distances in the optimized cluster range from 2.56 to 2.88 Å, with an average value of 2.72 Å. The distance in bulk Pt metal is 2.77 Å. The atoms in the center of the four faces are slightly puckered out from the center of the cluster.

The geometry of the optimized Pt_{10} cluster has Cs point-group symmetry. The absence of tetrahedral symmetry in this cluster is not unusual for small metal clusters. For example, Masel and co-workers used an embedded atom method to show that the lower energy structures of platinum clusters ranging from 5 to 60 atoms are disordered and show surface structures which are not present in bulk platinum [31]. Yang and co-workers have recently reported the existence of low symmetry geometries that are lower in energy than the icosahedral and cubo-octahedral structures [32].

The range of Pt–Pt distances found in the optimized cluster geometry is in agreement with experimental findings of Gallezot and Bergeret [18]. These authors determined from X-ray diffraction analyses that Pt clusters in Y-zeolite are distorted in the absence of adsorbates, and the interatomic distances are contracted with respect to the normal structure of bulk platinum. They also report a relaxation of the Pt clusters towards the Pt–Pt distance in bulk Pt, following adsorption of hydrogen and benzene. A wide variety of adsorbate-induced relaxations have been reported for small clusters [33–35]. This effect has been taken into account in the present study by allowing the entire cluster to optimize without imposing constraints, as described in the next section.

Boyanov and Morrison have studied the structures of platinum clusters containing 10–25 atoms on Y-zeolite, using X-ray absorption (XANES and EXAFS) and X-ray photoelectron spectroscopy [36]. They report the average interatomic distance to be 2.70 Å, and they conclude that this

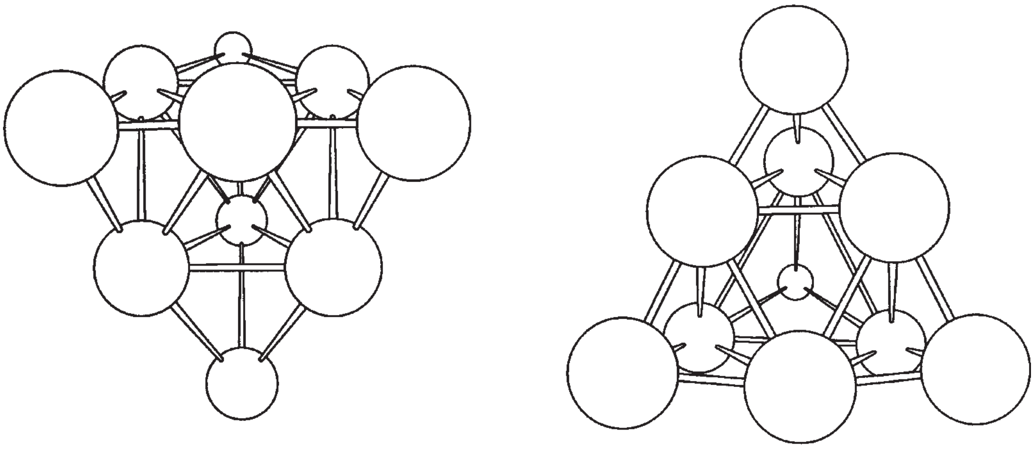

Figure 2. Two views of 10-atom platinum cluster.

bond contraction of 0.07 Å compared to bulk Pt is intrinsic to the cluster with no effect from zeolite support. Koningsberger and co-workers report from EXAFS measurements that the interatomic distance is 2.74 Å for a cluster of 4–5 Pt atoms with coordination number of 3.7 in L-zeolite [37]. Sachtler and co-workers have reported a value of 2.64 Å for platinum particles with average coordination number of 7.7 [38]. The results from these experimental studies are in agreement with the predictions from the present study that the average Pt–Pt distance of 2.72 Å in Pt_{10} clusters is shorter than the value of 2.77 Å in bulk Pt metal.

The chemical bonding energy of the Pt_{10} cluster with respect to Pt(d^9s^1) atoms is 2554 kJ/mol. The Pt–Pt bond strength is thus equal to 106 kJ/mol (since 24 Pt–Pt bonds are formed in the Pt_{10} cluster), compared to the value of 88 kJ/mol in bulk platinum metal [21]. The higher value of the average Pt–Pt bond strength for the Pt_{10} cluster is caused by the contribution from surface atoms of lower coordination (3 and 6) compared to the coordination of Pt in the bulk (12). The calculated average cohesive energy per Pt atom for the Pt_{10} cluster is 255 kJ/mol, while the bulk cohesive energy is 528 kJ/mol.

3.3. Density functional theory calculations: CO–Pt_{10}

Carbon monoxide adsorbs on one-fold (atop-sites) and two-fold (bridge-sites) positions on platinum surfaces. The optimized geometries for CO adsorption on Pt_{10} corresponding to the bridge and atop positions are shown in figures 3 and 4. The heat of adsorption on the atop-site is calculated to be 209 kJ/mol. The Pt–C and C–O bond lengths are 1.83 and 1.15 Å, respectively. The heat of CO adsorption on the bridge-site is calculated to be 142 kJ/mol, with Pt–C and C–O bond lengths of 1.97 and 1.18 Å, respectively. These values of 1.83 and 1.97 Å for the Pt–C distance at the atop- and bridge-sites are in agreement with LEED data which give Pt–C bond lengths of 1.85 (±0.1) Å and 2.08 (±0.07) Å, respectively [39]. Furthermore, the Pt–C distances in organoplatinum carbonyl compounds are 1.84–1.92 Å for terminal CO and 1.92–2.07 Å for bridged CO [40].

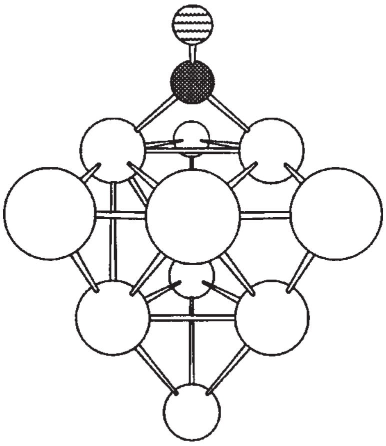

Figure 3. CO adsorption on bridge-site of Pt_{10} cluster. Open circle = Pt atom; filled circle = carbon atom; hatched circle = oxygen atom.

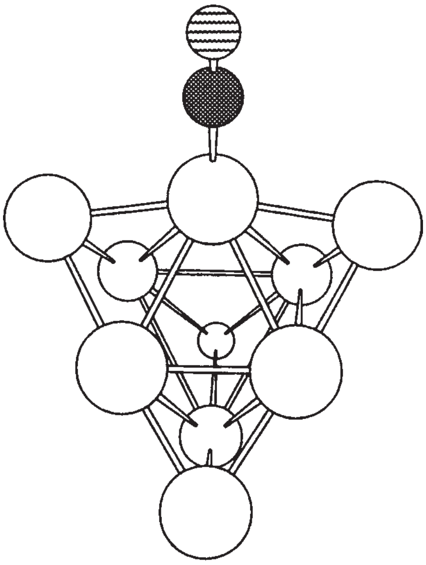

Figure 4. CO adsorption on atop-site of Pt_{10} cluster.

We have also calculated the heat of CO adsorption when two sites are occupied on the same Pt_{10} cluster. The heat of CO adsorption decreases from 209 to 197 kJ/mol

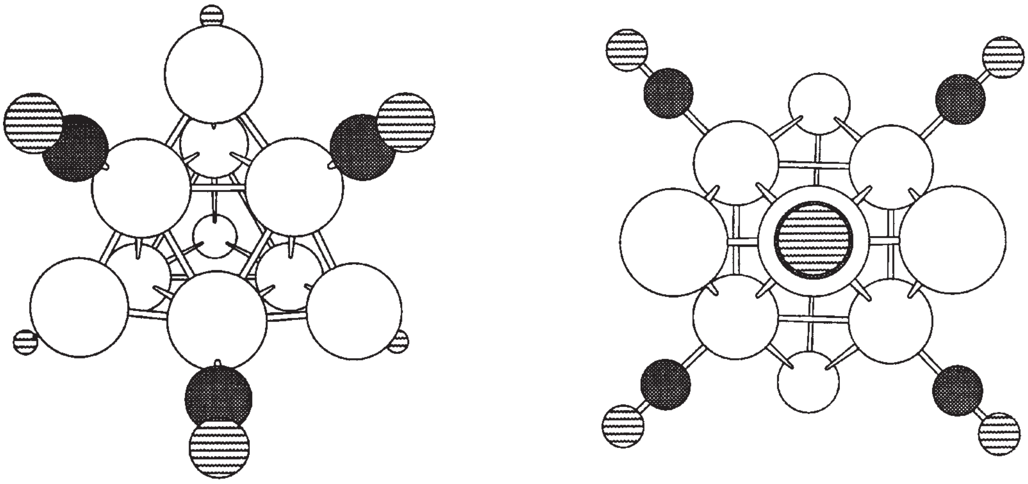

Figure 5. Adsorption of six CO molecules on atop-sites of Pt_{10} cluster.

when two atop-sites are occupied, while the heat decreases from 142 to 102 kJ/mol when two bridge-sites are occupied. Furthermore, the heat of CO adsorption decreases to 157 kJ/mol when six atop-sites are occupied on the same cluster, as shown in figure 5. At 403 K, the adsorption of CO on Pt/L-zeolite may not be equilibrated and hence the measured heat of adsorption, 125 kJ/mol, can be attributed to the high coverage of platinum by CO, in agreement with our theoretical results. Thus, the heat of CO adsorption on Pt/L-zeolite is predicted to decrease with adsorbate coverage, in agreement with our microcalorimetric results at 573 K.

As noted above, we do not expect our platinum particles to be disrupted and form Pt carbonyl species at the low CO pressures of this study. However, it is interesting to use DFT calculations to estimate the heat associated with this process. Specifically, we calculate the heat to be -30 kJ (endothermic) per mole of CO for the formation of neutral Pt–CO carbonyl clusters by reaction of Pt_{10} clusters with 10 molecules of CO. The prediction that this process in nearly neutral energetically is consistent with the experimentally observed disruption of Pt particles at high pressures of CO, especially when it is noted that the platinum carbonyl species undoubtedly gain stability upon interaction with the zeolite support.

We have corrected our calculated heat of CO adsorption at 0 K to compare with the measured heat at 573 K, by considering zero-point energy (ZPE) and thermal energies. To calculate thermal energy corrections, we assume that the adsorption process leads to a loss of one degree of translation and loss of two degrees of rotation. To calculate the ZPE we use the experimental values of C–O and Pt–C stretching frequencies, which are equal to 2080 and 475 cm^{-1} [41]. The ZPE for gas-phase CO molecule is calculated using the C–O stretching frequency of 2143 cm^{-1} [42]. The calculated heat of CO adsorption at 573 K is 211 kJ/mol, compared to 209 kJ/mol at 0 K. If we assume that the adsorption process leads to a loss of all three degrees of translation and loss of two degrees of rotation, the calculated heat of CO adsorption at 573 K is 216 kJ/mol. Hence the temperature correction for CO adsorption is small.

There seems to be disagreement in the literature regarding the energy difference between adsorption of CO on atop- and bridge-sites. A molecular orbital study using atom superposition and electron delocalization (ASED) showed the binding energy of CO on Pt(111) to be 180 kJ/mol for the atop-site and 120 kJ/mol for the bridge-site [43], in agreement with our results. Mieher and others have estimated the difference between these two sites to be only 0.62 kJ/mol [44]. At low coverage, Bradshaw and co-workers estimated that the atop-site is 6 kJ/mol more stable than the two-fold site [45], while Froitzheim and Schulze reported a difference of 30 kJ/mol [46]. Roszak and Balasubramanian have studied adsorption of CO on atop- and of bridge-sites on platinum dimers [47]. They show that the bridge-site is more stable than the atop-site by 46–96 kJ/mol, depending on the level of theory. We have carried out calculations of CO adsorption on Pt dimer using B3LYP theory and the LACVP** basis set. The ground state of the platinum dimer has multiplicity of three as there is an unpaired electron on each platinum atom. The ground state for bridged CO complex has no unpaired electrons, while the atop complex has a ground state with multiplicity of three which has a slightly lower energy than the singlet. We find that CO adsorption to form the bridged structure is more stable by 70 kJ/mol, in agreement with Roszak and Balasubramanian [47]. However, the opposite trend is seen with the Pt_{10} cluster, where the atop-site is more stable than the bridge-site by 70 kJ/mol. Indeed, several experimental studies have shown that only the atop-sites on Pt are occupied at low coverages, while population of the bridge-sites takes place on the Pt surface at fractional coverages above 0.14 [48–51].

According to Norskov and co-workers, the heat of CO adsorption on atop-sites of various Pt surfaces can be related to the position of the d-band of the Pt atop-atom relative to the Fermi energy [52]. Accordingly, we show in

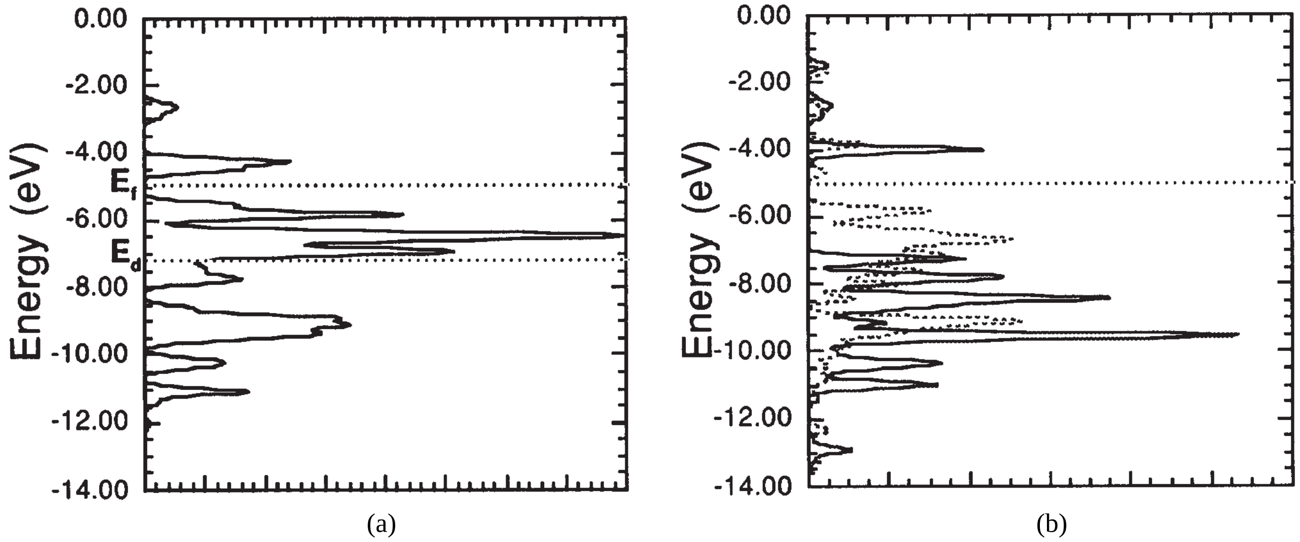

Figure 6. Platinum d-orbital density of states (a) before adsorption and (b) after CO adsorption; (- - -) bridge-site, (—) atop-site.

figure 6(a) the d-band density of states for the Pt atop-atom in the Pt_{10} cluster. The d-band center is 2.24 eV below the Fermi level, where the Fermi level of -4.99 eV has been taken to be the average of the HOMO and LUMO energies of the platinum cluster (-5.52 and -4.47 eV, respectively). According to the correlation of Norskov and co-workers, a d-band position of 2.24 eV relative to the Fermi energy corresponds to a heat of CO adsorption equal to 193 kJ/mol, in agreement with the value of 209 kJ/mol calculated in the present study. Thus, the same principles that control the heat of CO adsorption on bulk Pt surfaces (as studied by Norskov and co-workers) also seem to control adsorption on small Pt clusters (as studied in the present work). In agreement with this prediction, TPD analysis has shown that the desorption properties for CO on small particles of Pt on alumina are very similar to those for CO on bulk Pt [53]. We show in figure 6(b) the d-band density of states for the Pt atom in the Pt_{10} cluster after CO adsorption. The shift in the density of states to lower energy is more significant for adsorption of CO on atop-sites because of the stronger interaction of CO with the Pt_{10} cluster at this site.

We now speculate on the difference in energy for adsorption of CO on atop- and bridge-sites. We show in figures 7 and 8 the projection of the density of states for the sp and d orbitals of Pt onto the s and p_y orbitals of C, where the y-axis is normal to the Pt surface. It can be seen that the initially unoccupied sp orbitals of Pt near -3 eV overlap more extensively with the p_y orbital of the C atom at the atop-site. We conclude that there is more σ-donation from CO to Pt at the atop-site than the bridge-site, since there are more empty states available at the atop-site to accept electrons from CO. In addition, from figure 7 we see that there are more filled d-states near -9 eV that project onto the s and p_y orbitals of the C atom at the bridge-site than the atop-site. The filled states of Pt lead to repulsion interaction with the electrons of CO, and the adsorption of CO at the bridge-sites thus appears to be less favorable.

Because various authors have commented about the possible effects of electron transfer between platinum clusters and supports, we have also studied Pt_{10} clusters with a formal positive and negative charge, simulating electron-deficient and electron-rich species, respectively. Electron-deficient metal particles have been postulated to be the result of interaction with acid centers of zeolites [8,54–57]. Electron-rich metal particles can be attributed to the influence of basic oxygen atoms in zeolites or to the coadsorption of strong electropositive elements like potassium [58–60]. Interaction of CO with electron-deficient platinum atoms in zeolites has been investigated in a recent theoretical study by Rösch and co-workers [61].

The calculated structural parameters and heats of CO adsorption are presented for charged Pt clusters in table 1. The heat of CO adsorption at the atop-site is about the same for all the three species considered here. The C–O bond weakens as the cluster becomes more negative, which can be explained by more π-backdonation from the electron-rich cluster to CO. Weakening of the C–O bond is also evident in the calculated C–O stretching frequencies. The positions of the CO stretching frequencies have been reported to be influenced by several factors including, coverage effects, particle size effects, electron density changes induced by the catalyst support or cations, adsorption of CO on the matrix and structural rearrangement of platinum particles [29,62–70]. The calculated value of 2050 cm^{-1} for the neutral species is in agreement with the experimental values of 2040–2100 cm^{-1} for CO chemisorbed on atop-sites on platinum surfaces [49,71–74]. The C–O stretching frequency has been found to be sensitive to the metal surface coverage. Isotopic dilution experiments have shown that the frequency is 2050 cm^{-1} at vanishing coverage [68]. This frequency is in agreement with the value of 2050 cm^{-1} calculated for a single CO molecule adsorbed on the platinum cluster. At higher coverages the stretching frequency undergoes an upward shift to about 2080 cm^{-1} [68]. The cluster shown in figure 5 is representative of a highly cov-

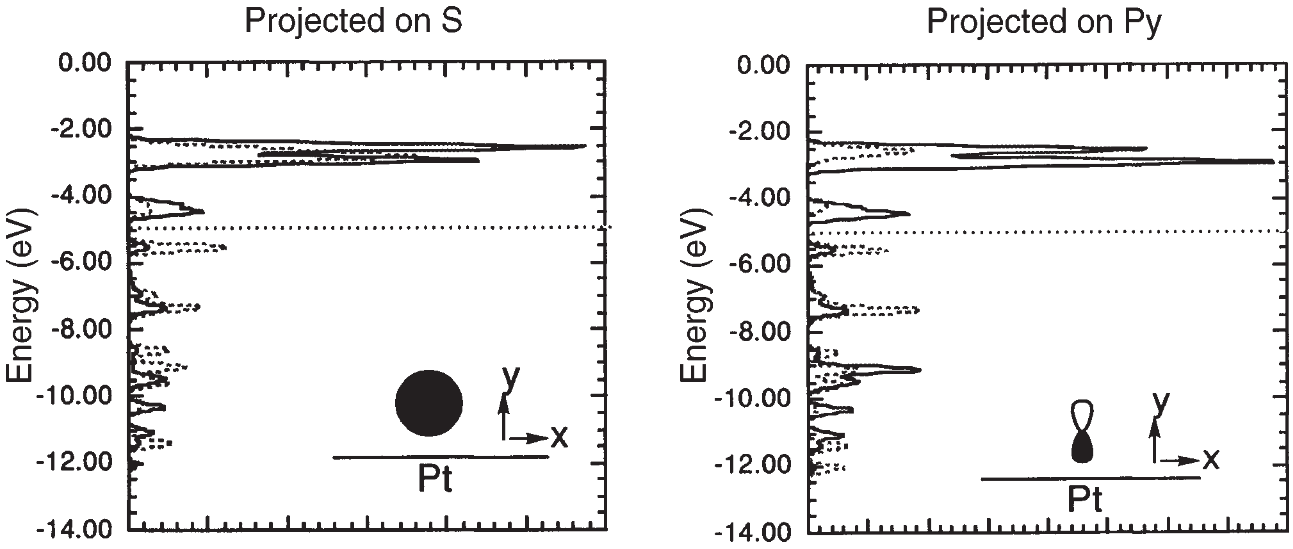

Figure 7. Platinum sp-orbital density of states projected on s and p_y orbitals of carbon; (- - -) bridge-site, (—) atop-site.

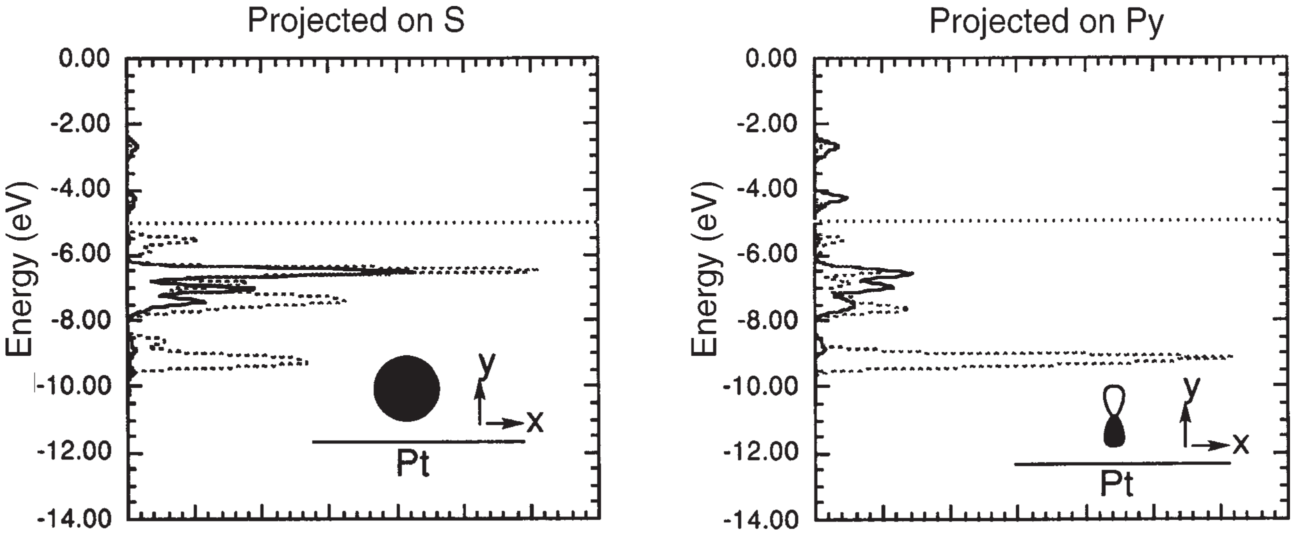

Figure 8. Platinum d-orbital density of states projected on s and p_y orbitals of carbon; (- - -) bridge-site, (—) atop-site.

Table 1
DFT results for CO adsorption on atop- and bridge-sites of Pt_{10} cluster.

Charge on Pt_{10} cluster	Atop-site			Bridge-site			Gas phase
	1	0	−1	1	0	−1	
ΔH_{ads} (kJ/mol)	227	209	221	138	142	181	
Pt–C (Å)	1.85	1.83	1.82	2.00	1.98	1.96	
C–O (Å)	1.14	1.15	1.16	1.17	1.18	1.19	1.13
C–O stretch (cm^{-1})	2120	2050	2020	1970	1850	1780	2143

ered surface. The C–O bond length in this cluster, where six CO molecules are adsorbed on the platinum cluster, is 0.007 Å shorter than the value for a single chemisorbed CO molecule. As we note from the table 1, the C–O stretching frequency is inversely proportional to the C–O bond length. Hence our results predict an upward shift of the C–O stretching frequency for the highly covered surface.

The experimental value for the stretching frequency of CO adsorbed on Pt clusters in neutralized L-zeolite is 2067 cm^{-1} [30], which indicates that these platinum clusters do not possess a significant charge. In contrast, bands near 2120 cm^{-1} have been reported for CO adsorbed on platinum clusters in acidic zeolites [69,75,76]. This band position agrees with our calculated value of 2120 cm^{-1} for the electron-deficient platinum cluster. On the other hand, a downward shift of the frequency with respect to Pt/SiO_2 has been reported for CO adsorption on platinum particles supported on basic K-L zeolite [29,62,67]. The low frequency band at 2030 cm^{-1}, assigned to the CO molecule adsorbed on electron-rich platinum particles, is in agreement with the calculated value of 2020 cm^{-1} for the CO adsorbed on the negatively charged platinum cluster. A broad band near 1850 cm^{-1} has been attributed to the bridge-bonded CO on various platinum surfaces [49,62,77,78]. The calculated value for the bridge-bonded CO on the neutral cluster is 1850 cm^{-1}, while we predict significant upward and downward shifts for the electron-deficient and electron-rich platinum clusters, respectively. As can be seen from table 1, the Pt–C distance decreases, the C–O distance increases, and the C–O stretching frequency decreases, as the charge on the platinum cluster becomes more negative. These observations are in agreement with a recent study of the Pt–C bond of CO adsorbed on small platinum particles supported in a NaX zeolite. This study concludes that the Pt–C stretching frequency is about 60 cm^{-1} higher, compared to larger particles and the authors attribute the stronger Pt–C bond to a negative charge on small platinum particles [79].

The heat of CO adsorption on bridge-sites for electron-rich clusters is significantly higher than that for neutral and electron-deficient clusters. For example, while CO adsorption is favored by 67 kJ/mol on the atop-sites for neutral Pt_{10}, it is favored by only 40 kJ/mol on negatively charged Pt_{10} clusters. This behavior can be attributed to increased backdonation from Pt to CO for these electron-rich clusters, since effects of backdonation are more important for bridge-sites compared to atop-sites [1,72]. This prediction may also be supported by experimental evidence that bridge-sites become increasingly occupied as electropositive potassium is co-adsorbed on platinum [60].

4. Conclusions

Carbon monoxide adsorption was studied on small platinum clusters using theoretical and experimental methods. The coverage effects and the electronic effects on the heats of adsorption as well as the C–O stretching frequencies were investigated for atop- and bridge-sites of adsorption. Density functional theory calculations show that CO linearly bonds on atop-sites and bridge-bonds on a clean Pt_{10} cluster with heats of adsorption of 209 and 142 kJ/mol, respectively. The higher heat for atop-sites can be explained by more σ-donation from CO to sp orbitals on Pt. Our results for CO adsorption on clusters agree with theoretical studies on extended metal surfaces, suggesting that CO adsorption is a local phenomenon and can be modeled using small metal clusters. Furthermore, our calculations indicate that the heat of adsorption of linearly bonded CO decreases from 209 to 157 kJ/mol as the CO coverage increases from one to six CO molecules per Pt_{10} cluster. Similarly, the heat of adsorption of bridge-bonded CO decreases from 142 to 102 kJ/mol as the number of bridge-bonded CO molecules increases from one to two per Pt_{10} cluster. Microcalorimetric measurements of CO adsorption at 573 K on L-zeolite-supported Pt give an initial heat of adsorption of 175 kJ/mol. These theoretical and experimental results are in general agreement, since at 573 K, the adsorption/desorption of CO is not completely equilibrated and the measured heat is the average heat of a highly covered Pt cluster. Electronic effects caused by electron transfer between Pt clusters and supports were addressed by studying CO adsorption on charged platinum clusters. We find that the bridge-site becomes more favorable on negatively charged platinum. The C–O stretching frequency observed experimentally for CO adsorption on Pt clusters in L-zeolite agrees with that calculated for neutral Pt clusters, suggesting that platinum clusters in this zeolite do not possess a significant charge. The calculated C–O stretching frequencies for the charged platinum clusters predict shifts in general agreement with experimental data.

Acknowledgement

We wish to acknowledge financial support for this work from the National Science Foundation and the National Center for Clean Industrial and Treatment Technologies.

References

[1] R.A. van Santen and M. Neurock, Catal. Rev. Sci. Eng. 37 (1995) 557.
[2] P.E.M. Siegbahn, Adv. Chem. Phys. XCIII (1996) 333.
[3] R.A. van Santen, in: *Chemisorption and Reactivity on Supported Clusters and Thin Films*, NATO ASI Series E: Applied Sciences, Vol. 331, eds. R.M. Lambert and B. Pacchioni (Kluwer, Dordrecht, 1997) p. 371.
[4] J.F. Paul and P. Sautet, Stud. Surf. Sci. Catal. 101 (1996) 1253.
[5] A. Fahmi and R.A. van Santen, J. Phys. Chem. 100 (1996) 5676.
[6] J.R. Bernard, in: *Proc. 5th Int. Conference on Zeolites* (Heyden, London, 1980) p. 686.
[7] L.M. Kustov, D. Ostgard and W.M.H. Sachtler, Catal. Lett. 9 (1991) 121.
[8] W.M.H. Sachtler and Z. Zhang, Adv. Catal. 39 (1993) 129.
[9] T.R. Hughes, W.C. Buss, P.W. Tamm and R.L. Jacobson, in: *New Development in Zeolite Science and Technology*, ed. Y. Murakami (Kodansha–Elsevier, Tokyo, 1986) p. 725.
[10] M. Che and C.O. Bennett, Adv. Catal. 36 (1989) 55.
[11] M. Vaarkamp, F.S. Modica, J.T. Miller and D.C. Koningsberger, J. Catal. 144 (1993) 611.
[12] B.L. Mojet and D.C. Koningsberger, Catal. Lett. 39 (1996) 191.
[13] M.N. Ringnalda, J.-M. Langlois, R.B. Murphy, B.H. Greeley, C. Cortis, T.V. Russo, B. Marten, R.E.J. Donnelly, W.T. Pollard, Y. Cao, R.P. Muller, D.T. Mainz, J.R. Wright, G.H. Miller, W.A. Goddard III and R.A. Friesner, PS-GVB V. 2.3 (Schrodinger, Inc., 1996).
[14] A.D. Becke, J. Chem. Phys. 98 (1993) 5648.
[15] P.J. Hay and W.R. Wadt, J. Chem. Phys. 82 (1985) 299.
[16] W.J. Hehre, L. Radom, P.V.R. Schleyer and J.A. Pople, *Ab Initio Molecular Orbital Theory* (Wiley, New York, 1987).
[17] P. Gallezot, Surf. Sci. 106 (1981) 459.
[18] P. Gallezot and G. Bergeret, J. Catal. 72 (1981) 294.
[19] B. Moraweck, G. Clugnet and A.J. Renouprez, Surf. Sci. 81 (1979) L631.
[20] S.F. Boys and F. Bernardi, Mol. Phys. 19 (1970) 553.
[21] R.C. Weast, ed., *Handbook of Chemistry and Physics* (CRC, Boca Raton, FL, 1989).
[22] Z. Hong, B.E. Handy, B.E. Spiewak and J.A. Dumesic, Thermochim. Acta, submitted.
[23] B.E. Spiewak, J. Shen and J.A. Dumesic, J. Phys. Chem. 99 (1995) 17640.
[24] B.E. Spiewak and J.A. Dumesic, Thermochim. Acta 290 (1997) 43.
[25] S.B. Sharma, J.T. Miller and J.A. Dumesic, J. Catal. 148 (1994) 198.
[26] Y.Y. Yeo, L. Vattuone and D.A. King, J. Chem. Phys. 104 (1996) 3810.
[27] C.E. Wartnaby, A. Stuck, Y.Y. Yeo and D.A. King, J. Phys. Chem. 100 (1996) 12483.
[28] Y.Y. Yeo, L. Vattuone and D.A. King, J. Chem. Phys. 106 (1997) 392.
[29] A.Y. Stakheev, E.S. Shpiro, N.I. Jaegar and G. Schulz-Ekloff, Catal. Lett. 34 (1995) 293.

[30] S.B. Sharma, T.E. Laska, P. Balaraman, T.W. Root and J.A. Dumesic, J. Catal. 150 (1994) 225.

[31] A. Sachdev, R.I. Masel and J.B. Adams, J. Catal. 136 (1992) 320.

[32] S.H. Yang, D.A. Drabold, J.B. Adams, P. Ordejon and K. Glassford, J. Phys. Condens. Matter 9 (1997) L39.

[33] G.A. Somorjai, *Introduction to Surface Chemistry and Catalysis* (Wiley, New York, 1994).

[34] M.A. Van Hove and G.A. Somorjai, Surf. Sci. 299/300 (1994) 487.

[35] M.C.J. Bradford and M.A. Vannice, Ind. Eng. Chem. Res. 35 (1996) 3171.

[36] B.I. Boyanov and T.I. Morrison, J. Phys. Chem. 100 (1996) 16310.

[37] M. Vaarkamp, B.L. Mojet, M.J. Kappers, J.T. Miller and D.C. Koningsberger, J. Phys. Chem. 99 (1995) 16067.

[38] M.S. Tzou, B.K. Teo and W.M.H. Sachtler, J. Catal. 113 (1988) 220.

[39] D.F. Ogletree, M.A. Van Hove and G.A. Somorjai, Surf. Sci. 173 (1986) 351.

[40] G. Wilkinson, F.G.A. Stone and E.W. Abel, *Comprehensive Organometallic Chemistry*, Vol. 6 (Pergamon Press, New York, 1982).

[41] H. Froitzheim, H. Hopster, H. Ibach and S. Lehwald, Appl. Phys. 13 (1977) 147.

[42] G. Herzberg, *Molecular Spectra and Molecular Structure I. Spectra of Diatomic Molecules* (Nostrand, New York, 1950).

[43] N.K. Ray and A.B. Anderson, Surf. Sci. 119 (1982) 35.

[44] W.D. Mieher, L.J. Whitman and W. Ho, J. Chem. Phys. 91 (1989) 3228.

[45] E. Schweizer, B.N.J. Persson, M. Tushaus, D. Hoge and A.M. Bradshaw, Surf. Sci. 213 (1989) 49.

[46] H. Froitzheim and M. Schulze, Surf. Sci. 212 (1989) 837.

[47] S. Roszak and K. Balasubramanian, J. Chem. Phys. 103 (1995) 1043.

[48] N. Sheppard and T.N. Nguyen, in: *Advances in Infrared and Raman Spectroscopy*, eds. R.J.H. Clark and R.E. Hester (Hayden, London, 1978) p. 67.

[49] B.E. Hayden and A.M. Bradshaw, Surf. Sci. 125 (1983) 787.

[50] M. Song, K. Yoshimi and M. Ito, Chem. Phys. Lett. 263 (1996) 585.

[51] J. Yoshinobu and M. Kawai, Surf. Sci. 363 (1996) 105.

[52] B. Hammer, O.H. Nielsen and J.K. Norskov, Catal. Lett. 46 (1997) 31.

[53] E.I. Altman and R.J. Gorte, Surf. Sci. 172 (1986) 71.

[54] P. Gallezot, Catal. Rev. Sci. Eng. 20 (1979) 121.

[55] W. Juszczyk, Z. Karpinski, I. Ratajczykowa, Z. Stanasiuk, J. Zielinski, L.L. Sheu and W.M.H. Sachtler, J. Catal. 120 (1989) 68.

[56] R.A.D. Betta and M. Boudart, in: *Proc. 5th Int. Congress on Catalysis*, ed. H. Hightower (North-Holland, Amsterdam, 1973) p. 1329.

[57] M.G. Samant and M. Boudart, J. Phys. Chem. 95 (1991) 4070.

[58] D.J. Barthomeuf, J. Phys. Chem. 88 (1984) 42.

[59] G. Larsen and G.L. Haller, Catal. Lett. 3 (1989) 103.

[60] E.L. Garfunkel, J.E. Crowell and G.A. Somorjai, J. Phys. Chem. 86 (1982) 310.

[61] A.L. Yakovlev, K.M. Neyman, G.M. Zhidomirov and N. Rösch, J. Phys. Chem. 100 (1996) 3482.

[62] G.S. Lane, J.T. Miller, F.S. Modica and M.K. Barr, J. Catal. 141 (1993) 465.

[63] M.J. Kappers, M. Vaarkamp, J.T. Miller, F.S. Modica, M.K. Barr, J.H. van der Maas and D.C. Koningsberger, Catal. Lett. 21 (1993) 235.

[64] M.J. Kappers, J.T. Miller and D.C. Koningsberger, J. Phys. Chem. 100 (1996) 3227.

[65] R.A. Dalla Betta, J. Phys. Chem. 79 (1975) 2519.

[66] W.H. Han, A.B. Kooh and R.F. Hicks, Catal. Lett. 18 (1993) 193.

[67] P.V. Menacherry and G.L. Haller, Catal. Lett. 44 (1997) 135.

[68] M. Primet, J. Catal. 88 (1984) 273.

[69] A.Y. Stakheev, E.S. Shpiro, O.P. Tkachenko, N.I. Jaeger and G. Schulz-Ekloff, J. Catal. 169 (1997) 382.

[70] F.J.C.M. Toolenaar, A.G.T.M. Bastein and V. Ponec, J. Catal. 82 (1983) 35.

[71] G. Ertl, M. Neumann and K.M. Streit, Surf. Sci. 64 (1977) 393.

[72] V.F. Kiselev and O.V. Krylov, in: *Adsorption and Catalysis on Transition Metals and Oxides*, Springer Series in Surface Science, eds. G. Ertl and R. Gomer (Springer, New York, 1989).

[73] C. Klünker, M. Balden, S. Lehwald and W. Daum, Surf. Sci. 360 (1996) 104.

[74] H. Steininger, S. Lehwald and H. Ibach, Surf. Sci. 123 (1982) 264.

[75] V.L. Zholobenko, G.D. Lei, B.T. Carvill, B.A. Lerner and W.M.H. Sachtler, J. Chem. Soc. Faraday Trans. 90 (1994) 233.

[76] O.P. Tkachenko, E.S. Shpiro, N.I. Jaeger, R. Lamber, G. Schulz-Ekloff and H. Landmesser, Catal. Lett. 23 (1994) 251.

[77] R.D. Eichens and W.A. Pliskin, Adv. Catal. 10 (1958) 1.

[78] H. Ibach and D.L. Mills, *Electron Energy Loss Spectroscopy and Surface Vibration* (Academic Press, New York, 1982).

[79] V.B. Kazansky, V.Y. Borovkov, N. Sokolova, N.I. Jaeger and G. Schulz-Ekloff, Catal. Lett. 23 (1994) 263.